Evaluating the Impact of Model Physics on HWRF Forecasts of Tropical Cyclone Rapid Intensification

Jun A. Zhang

NOAA/Hurricane Research Division with University of Miami/CIMAS

(Email: jun.zhang@noaa.gov)

Final Project Report Developmental Testbed Center (DTC) Visitor Program 2017

December 2018

1. Background

Improving the intensity and track forecasts of tropical cyclones (TCs) with Rapid Intensification (RI) is important because under-prediction of RI could lead to a heavy toll of human lives and significant financial loss, especially if a TC with RI makes landfall at well-developed coastal cities. However, forecasting TC RI has remained a big challenge for forecasters who rely on numerical models, because of the deficiency in TC models to reproduce the physical processes.

Unlike hurricane track, which is primarily determined by the environmental flows, hurricane intensity is controlled by the interactions between the environmental factors and the vortex itself. Using data from the operational Statistical Hurricane Intensity Prediction Schemes (SHIPS) model, Kaplan et al. (2010; 2015) showed that systems that undergo RI are situated in regions with lower vertical shear of the horizontal wind, greater upper-level divergence, and higher low-level relative humidity than those that do not (Fig. 1). Their results also suggest that about 35% of the skill of predicting RI for the Atlantic basin[1] is captured by processes that are controlled by the large-scale environment since only information from those scales are employed in the rapid intensity index. Thus, it is hypothesized that the remainder of the skill is dependent on inner core dynamics and upper ocean interactions, given the limitation of the predictability.

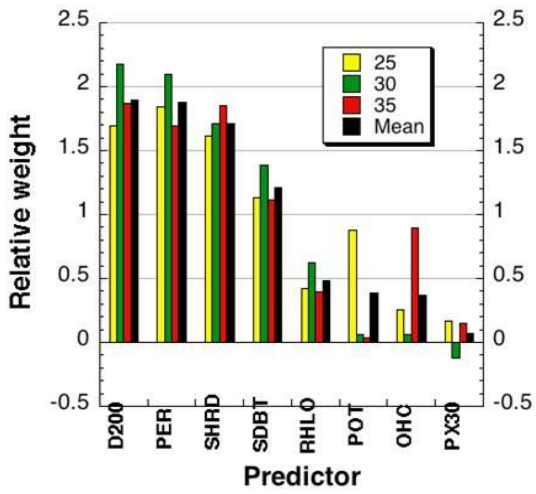

Figure 1: Relative weights of the Atlantic Ocean basin rapid intensification (RI) index predictors for 25-kt (yellow), 30-kt (green), and 35-kt (red) 24-h RI thresholds. Mean weights (black) of all three RI thresholds are also shown for the RI predictors. The predictors are the 850-200 hPA vertical shear of the horizontal wind (SHRD), 200 hPA divergence (D200), 850-200 hPA low-level relative humidity (RHLO), surface potential intensity (POT), oceanic heat content (OHC), areal coverage of $\leq$-30ºC infrared brightness temperature between 50-200 km radius (PX30), standard deviation of infra-red brightness temperatures over that same region (SDBT), and previous 12-h intensity change (PER). This Figure is from Kaplan et al. (2010).

[1]RI, in this context, is defined as an increase in hurricane intensity (measured by the maximum 1-min sustained 10-m wind speed) by a minimum of 30 kt within a 24-hour period.

While it is widely recognized that TC asymmetric dynamics play an important role in intensity change, the theoretical study by Nolan et al. (2007) demonstrated that the TC symmetric response to the azimuthally averaged heating, which dominates the symmetric response to the heating associated with individual asymmetries, is also responsible for the resulting intensity change. By analyzing the microwave remote sensing of TCs undergoing RI, recent observational studies (Kieper and Jiang 2012) showed the majority of RI cases have a symmetric eyewall prior to RI onset. The observational studies (e.g., Kossin and Eastin 2001; Rogers et al. 2013) showed that all intensifying storms have ring-like vorticity structure while non-intensifying storms have a monopole-like vorticity structure. Previous studies that examined the energy efficiency in TCs suggest that small eye size (Hack and Schubert 1986) and high-altitude warm core (Zhang and Chen 2012) favor RI.

What remains the most challenging in RI forecasts is to realistically represent the inner-core processes in the physical packages. Of note, most of physics schemes were initially designed for coarse resolution and non-TC conditions. As the horizontal resolution of the operational hurricane forecast models (e.g., HWRF) approaches 2 km (and may eventually reach 1 km), physical parameterizations traditionally used with low-resolution operational models may be inappropriate. Thus, physical parameterizations need to be evaluated comprehensively in the context of RI for their use to be justified. For this project, we studied how model physics impacts the RI forecast in HWRF.

2. Objectives

The goal of this project is to evaluate the model performance of the HWRF model in forecasting RI that is tied to different model physics. Specifically, we aim to evaluate the impact of the following components of the model physics on HWRF RI forecasts:

1) Horizontal diffusion parameterization.
2) Cumulus parameterization.
3) Boundary-layer parameterization.

3. Summary of Results

For this project, we used retrospective HWRF forecasts of TCs from both EMC and DTC. For each task that corresponds to the related objective listed above for each model physics component,

we group the HWRF retrospective forecasts into four groups - captured RI (Hit), missed RI (Miss), predicted RI with false alarm (False Alarm), and correctly rejected RI events, based on their RI performance. We show the RI verification in a contingency table (Table 1). For a given component of model physics that shows substantial improvement in the RI forecast in terms of Critical Success Index (CSI), we conducted detailed analysis of the TC structure and dynamics to understand why the change in model physics makes the RI forecast better. Note that the CSI is defined as the ratio of the number of Hits to the total number of Hits, False Alarms, and Misses.

		Observed	
		Yes	**No**
Forecast	**Yes**	Hit	False Alarm
	No	Miss	Correct Rejection

Table 1. Sample contingency table for RI verification.

Task 1. Assessment of HWRF performance in forecasting RI with different setup of horizontal mixing length

In this task, we used retrospective HWRF forecasts from EMC. During the HWRF upgrade o in 2016, the horizontal mixing length, L_h, was reduced following observations of Zhang and Montgomery (2012) and numerical simulations of Bryan et al. (2010). EMC ran two sets of retrospective forecasts of 10 TCs: one using the operational H216 HWRF in which L_h was set to 800 m (referred to as HOAC hereafter) and the other using H216 but with L_h set to 1900 m (i.e., the value as in H215, referred to as COAC hereafter).Verification of the track and intensity forecasts against NHC's best track data showed that there is no significant improvement or downgrade for track forecast, but there is a significant improvement in intensity forecast at 80% confidence interval at lead times of 6–30, 40–60, and 84–120 h. Significant improvement was also found in the intensity bias and storm size in terms of radius of the maximum wind speed. This result has been reported by Zhang et al. (2018). We further evaluate the impact of horizontal diffusion on RI forecast by creating a contingency table as mentioned earlier. It is evident from Table 2 that there is no substantial improvement in the RI forecast when reducing

L_h in HWRF. The CSI is actually slightly reduced from 0.03 to 0.02. This result did not change much when we changed the RI threshold from 30 kt to 20 kt change in 24 h.

HOAC	**Observed**		
Forecast		Yes	No
	Yes	1	41
	No	9	371

Table 2. Contingency table for HWRF predictions of RI for HOAC (L_h=800 m).

COAC	**Observed**		
Forecast		Yes	No
	Yes	1	19
	No	10	392

Table 3. Contingency table for HWRF predictions of RI for COAC (L_h=1900 m).

Task 2. Assessment of HWRF performance in forecasting RI with different cumulus parameterizations

In this task, we used retrospective HWRF forecasts from DTC. The cumulus parameterization scheme developed by Grell and Freitas (2014, GF scheme hereafter) has been added to the trunk of HWRF by DTC for potential operational use. Biswas et al. (2014) tested the sensitivity of HWRF track and intensity forecasts to the Arakawa-Schubert Scheme (SAS) used in the operational HWRF and the GF scheme and found large differences in forecasts. Using the 2016 version HWRF (H216), DTC created additional retrospective forecasts to further evaluate the role of the cumulus schemes on RI forecasts. Of note, both the SAS (Arakawa and Schubert 1974; Arakawa and Wu 2013) and GF scheme have the scale-aware feature. But their parameterizations of heating relative to the microphysics impact is different, with the SAS scheme contribution to the total heating being larger than the GF scheme in the inner most domain. DTC run a total of 128 homogeneous cases between the HWRF forecasts with the SAS scheme (H6CL) and those with the GF scheme (H6GF). Here we focus on RI verification using

the contingency table. Tables 4 and 5, respectively, summarize the verification result for H6CL and H6GF, showing the probability detection rate is improved in H6GF compared to H6CL, although the false alarm ratio is enlarged in H6GF. Overall, the CSI score is improved from 0.3 for H6CL to 0.36 for H6GF.

H6CL	**Observed**		
Forecast		Yes	No
	Yes	28	13
	No	52	472

Table 4: Contingency table for HWRF predictions of RI for H6CL.

H6CL	**Observed**		
Forecast		Yes	No
	Yes	38	26
	No	42	459

Table 5: Contingency table for HWRF predictions of RI for H6GF.

To understand why H6GF did better job in terms of RI forecast than H6CL, a case study approach is used here. HWRF forecasts of Hurricane Gonzalo (2014) initialized at 12 UTC 13 October are analyzed. The track and intensity forecasts from H6CL and H6GF along with the Best Track are shown in Fig. 2, indicating similar track forecasts but a much better intensity forecast in H6GF than in H6CL. To verify performance of two forecasts in terms of TC structure, we compare the 2-km altitude wind speed from the two forecasts to the Doppler radar observations (Fig. 3). It is shown that in terms of both the maximum wind speed and storm size, H6GF performed much better than H6CL compared to the radar observations. Although both forecasts captured the asymmetric distribution of the wind field, the wind speed is too weak in the H6CL forecast.

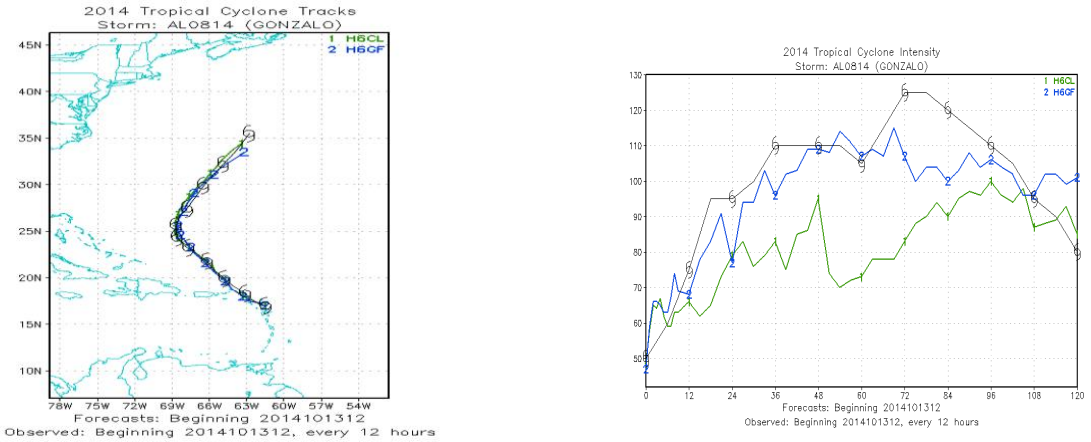

(a) (b)

Figure 2: HWRF forecasts of Hurricane Gonzalo (2014) with SAS and GF cumulus schemes, denoted as H6CL (blue) and H6GF (green), respectively. The left panel shows the track forecasts and the right panel shows the intensity forecasts. The black line is from the Best Track data.

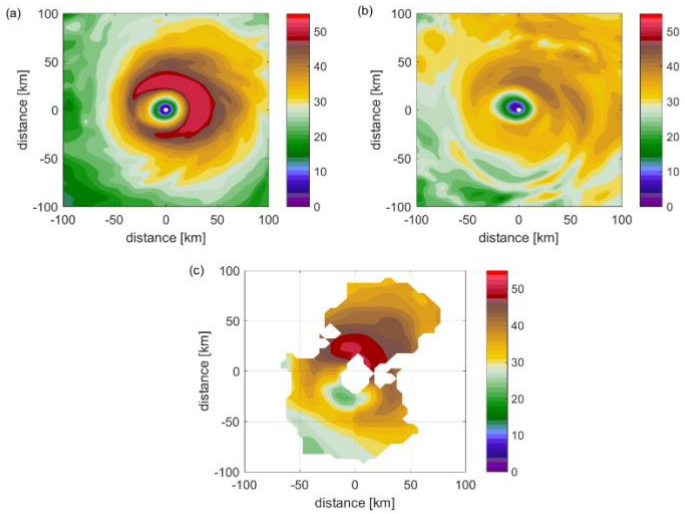

Figure 3: Horizontal view of 2-km wind speed from (a) H6GF forecast, (b) H6CL forecast, and Doppler radar observation, validated at lead time of 48 h.

TC structure at the RI onset before the intensity bifurcation point was compared between the two forecasts. Angular momentum budget was also conducted. Detailed results are reported in paper to be submitted to Weather and Forecasting (Biswas et al. 2019). Overall, we found that the inflow strength is much larger in the boundary layer in the H6GF forecast than in the H6CL forecast. The vortex is also deeper and stronger in the H6GF forecast than in the H6CL forecast. This enhanced inflow makes the convergence of the angular momentum larger in the H6GF forecast, resulting in faster intensification in the H6GF forecast, in agreement with the TC spin-

up theory (Smith et al. 2009). The temperature tendency was also compared between the two forecasts, showing that the cumulus contribution to the temperature tendency is smaller in the H6GF forecast than in the H6CL forecast. This may help explain the inner core temperature and moisture differences between the two forecasts. The inner-core region has larger humidity in the H6GF forecast than in the H6CL forecast, especially in the boundary layer. Zhang et al. (2017) and Kieu et al. (2014) also showed that more rapidly intensifying TCs tend to have more moist boundary layers. Overall, our analyses further confirm the GF scheme performed better in HWRF RI forecasts than the SAS scheme.

Task 3. Assessment of HWRF performance in forecasting RI with different boundary-layer parameterization schemes

In this task, we used retrospective HWRF forecasts from EMC. Two sets of HWRF retrospective forecasts of over 120 cases were conducted by EMC with α=0.5 (referred to as lowKm hereafter) and α=1 (referred to as highKm hereafter), respectively, in a cycling mode, using the same initial conditions at the first forecast. Here α is a tuning parameter controlling the magnitude of vertical eddy diffusivity (K_m). K_m calculated using α=0.5 better matches with observational estimates given by Zhang et al. (2011) and Zhang and Drennan (2012) than that calculated using α=1 as in the earlier version of the HWRF model (see Fig. 1 of Zhang et al. 2017). Tables 6 and 7 summarize the result of the RI verification for highKm and lowKm forecasts, respectively. It is evident that reducing eddy diffusivity in HWRF planetary boundary layer (PBL) scheme substantially improved the RI forecast with much larger probability detection rate. Although the false alarm ratio is larger in the lowKm forecast than in the highKm forecast, the overall CSI score is much larger in the lowKm forecast (0.62) than the highKm forecast (0.22).

highKm	**Observed**		
Forecast		Yes	No
	Yes	4	0
	No	14	202

Table 6: Contingency table for HWRF predictions of RI for H6CL.

H6CL	**Observed**		
Forecast		Yes	No
	Yes	16	8
	No	2	194

Table 7: Contingency table for HWRF predictions of RI for H6GF.

The composite analysis of the TC structure at the RI onset of the two sets of HWRF forecasts with different PBL parameterizations was documented by Zhang et al. (2017). Here in this project we focused on analyzing two HWRF forecasts of Hurricanes Earl (2010) that are initiated at 12 UTC on 27 August 2010: one from highKm and the other from lowKm forecasts. The storm intensity from these two forecasts, as measured by the peak 10-m wind speed (V_{max}), is shown in Fig. 4. It appears that the storm intensity is similar between the two forecasts in the first 36 h, slowly intensifying up to the bifurcation point at t=54 h when the storm in the highKm forecast weakens briefly before resuming a slow intensification, while the storm intensifies in the low-Km forecast until t=84 h when peak intensity is reached. The intensity forecast in the lowKm run follows the best-track intensity much better than the highKm forecast.

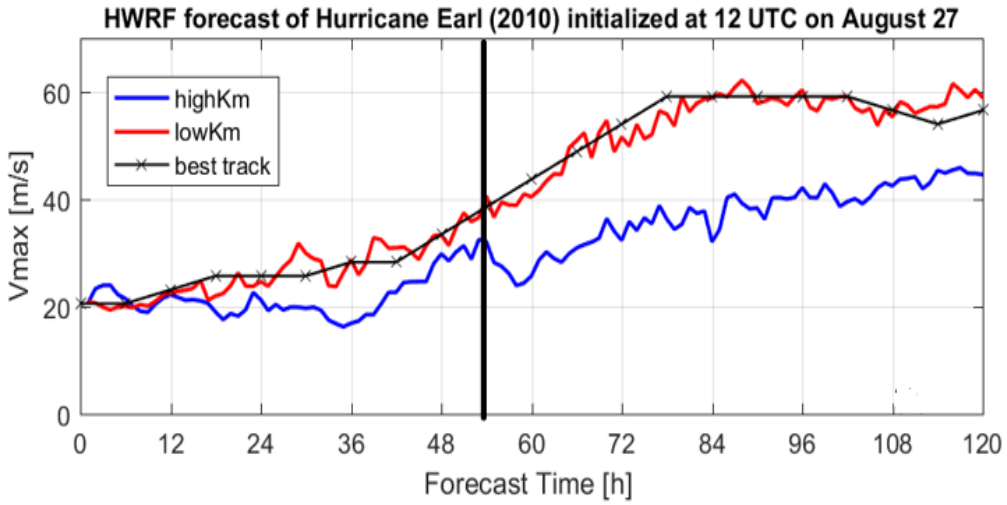

Figure 4: Plot of the maximum wind speed from highKm (blue) and lowKm (red) forecasts of Hurricane Earl (2010) compared to the Best Track (black).

We focused on evaluating how K_m affects four physical processes that are related to RI: 1) angular momentum convergence, primarily by the mean flow; 2) location of convective bursts; 3) vortex tilt/precession; and 4) air-sea fluxes and PBL recovery, which is related to the tilt evolution. Detailed comparisons between the two Earl forecasts are reported in a paper accepted in *Monthly Weather Review* (Zhang and Rogers 2019).

Our result suggests that the lower K_m leads to stronger inflow and boundary-layer convergence, and stronger updrafts that are also closer to the storm center. Dynamically, the hurricane vortex in the lowKm forecast is much stronger and deeper due to the stronger convergence of angular momentum that offsets the friction-induced dissipation. A stronger vortex is then more resilient to shear from being tilted. It is evident from Fig. 5a that the low-level and upper-level vortices tend to align after the spin-up period in the lowKm forecast, while a precession of the vorticies occurs in the highKm forecast after the intensity bifurcation point indicated by the black line. It is also found that the hurricane vortex in the lowKm forecast has smaller static stability above the boundary layer, which makes it more resilient to shear than the vortex in the highKm forecast (Fig. 5b), according vortex tilt theory (Jones 1995; Reasor et al. 2004; Schecter 2015).

(a)

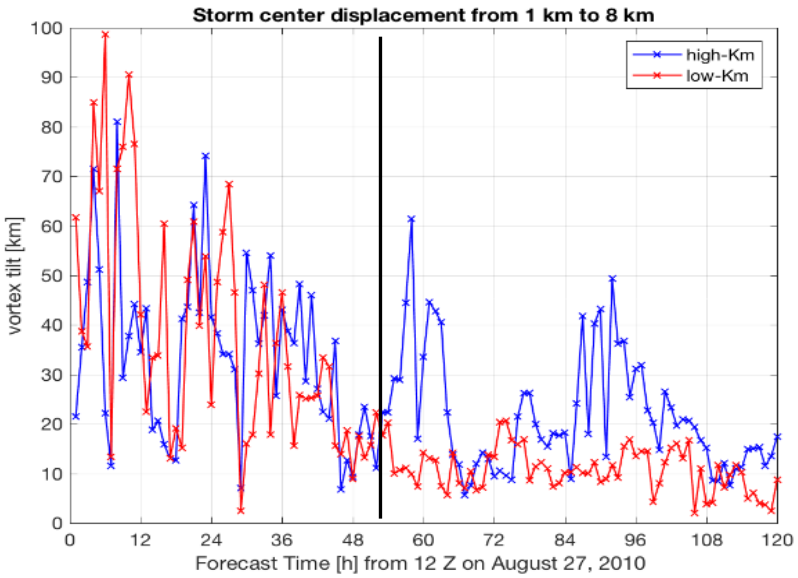

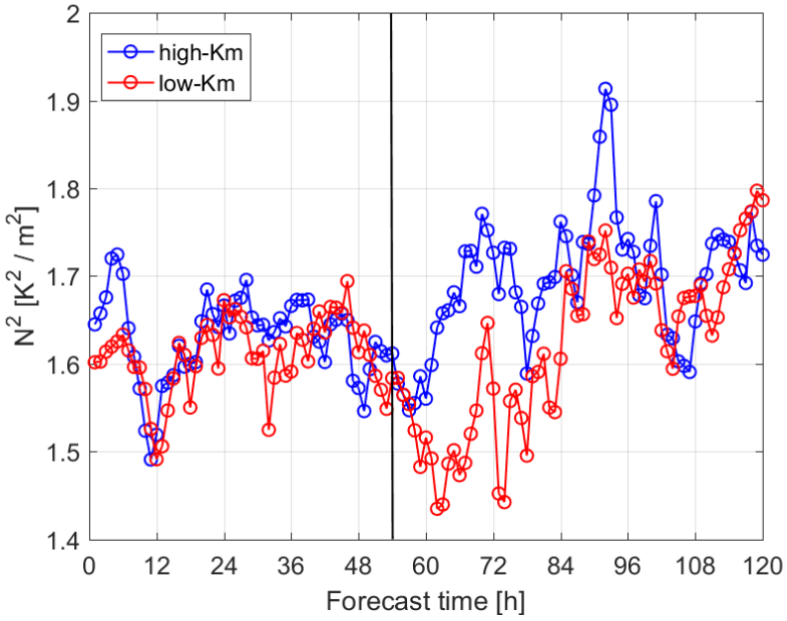

(b)

Figure 5: Plot of the evolution of (a) vortex tilt (1-8 km) and (b) static stability above the boundary layer for highKm (blue) and lowKm (red) forecasts. The black line indicates the bifurcation point.

The more symmetric deep convection (Fig. 6) may also contribute to the alignment of the vortex in the lowKm composite following Braun et al. (2006) and Rogers et al. (2015). The radial locations of deep convection as indicated by convective bursts are also modulated by the boundary-layer K_m. This modulation supports the idea that TCs with convective bursts located inside the low-level RMW, which preferentially occur for reduced K_m, are more favorable for RI than TCs with convective bursts located primarily outside the RMW.

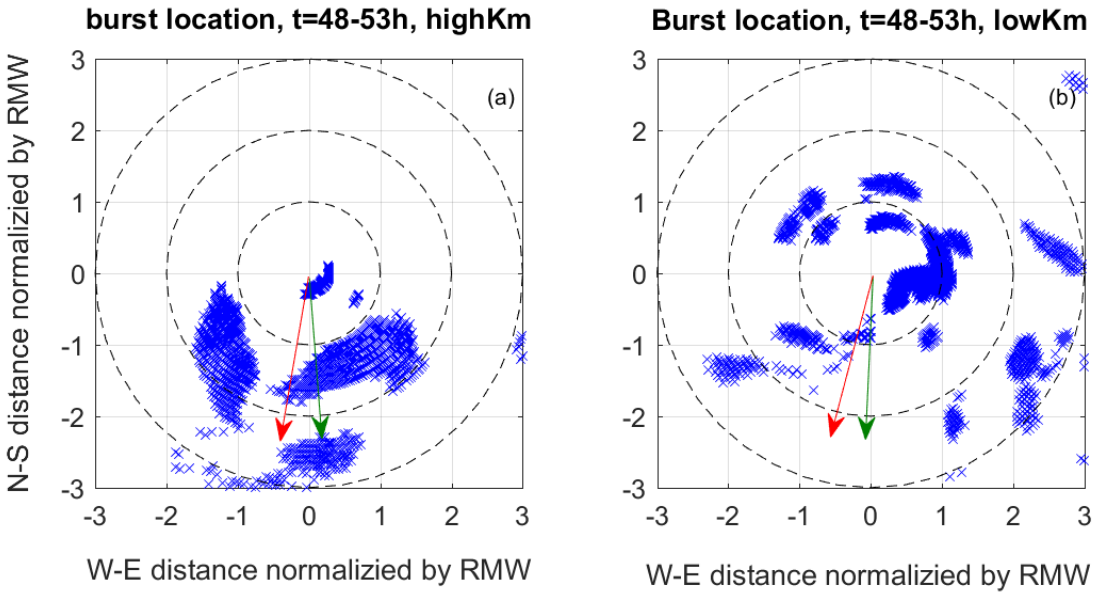

Figure 6: Horizontal view of convective bursts during the period between 48 and 53 h of forecast time for highKm (a) and lowKm (b) forecasts of Hurricane Earl (2010). The red arrow indicates the shear direction and the green arrow indicates the tilt direction.

We also compared the thermodynamic structure in the boundary layer between the two forecasts. We found that when the vortex tilt is larger in the highKm forecast, the boundary-layer θ_e is much smaller than that in the lowKm forecast after the intensity bifurcation point (Fig. 7). Consistent with previous studies, we found convective downdrafts bring down low-θ_e air from above the boundary layer in the downshear and downshear left quadrants where the vortex tilt also occurs (Riemer et al. 2010; Zhang et al. 2013). With larger tilt, more low values of θ_e are flushed into the boundary layer in the highKm forecast, which can not be recovered by surface enthalpy fluxes as the air parcel spirals inward from the outer core to the eyewall region following an inflow trajectory. On the other hand, surface enthalpy fluxes are enough to recover the deficit of θ_e in the lowKm forecast.

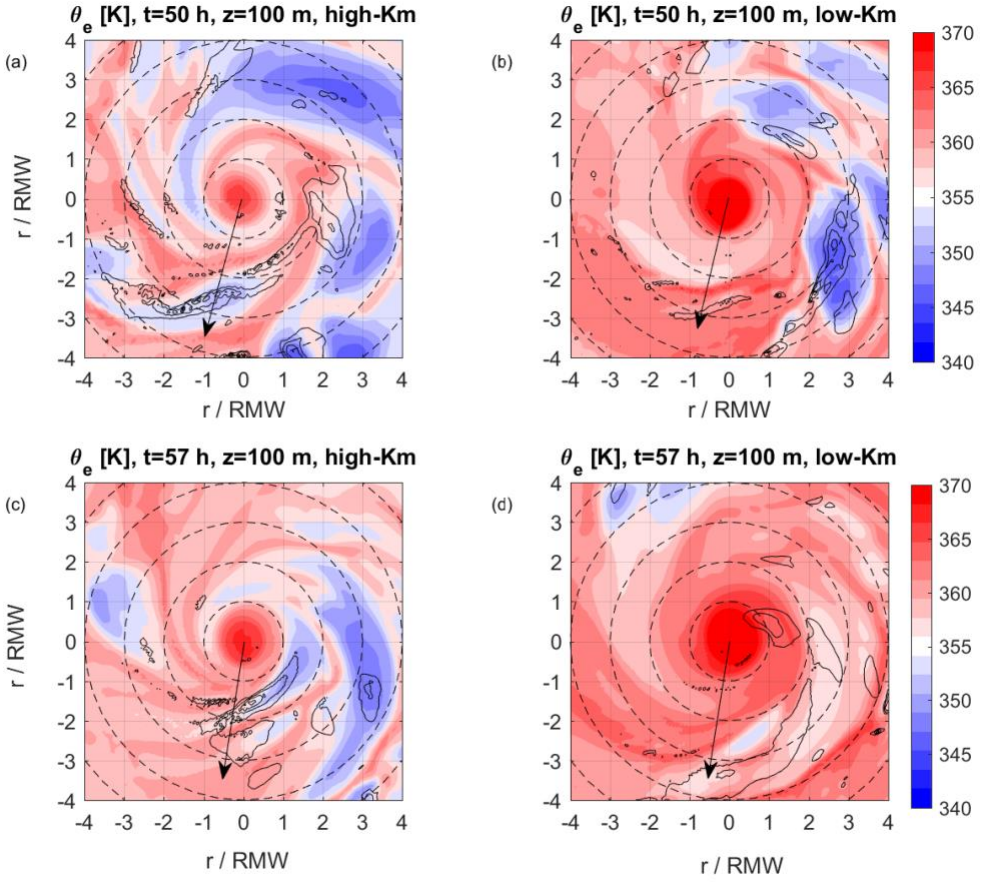

Figure 7: Horizontal view of the equivalent potential temperature (θ_e, shading) at 100 m altitude and vertical velocity at 1.5 km altitude (contours) at t=50 h (upper panels) and t=57 h (lower panels). The left and right panels are from the highKm and lowKm forecasts, respectively. The black arrow shows the shear direction. Note that only downward motion (negative vertical velocity) is shown with contour interval of 0.2 ms^{-1}.

4. Conclusions and future work:

In this project, we evaluated the impact of model physics on HWRF forecasts of hurricane rapid intensification (RI) using retrospective forecasts. We found that both cumulus and boundary layer schemes have substantial impact on HWRF's RI prediction, while the impact of horizontal diffusion parameterization is small. The case study of Hurricane Gonzalo (2014) shows that the GF cumulus scheme performs better in terms of hurricane structure forecast in HWRF, which is tied to a better RI forecast than the SAS scheme. The case study of Hurricane Earl (2010) shows that boundary layer eddy diffusivity regulates not only the boundary layer structure but also the vortex-scale and convective-scale structure and their interaction with environmental wind shear.

This multiscale interaction process is important for RI prediction and should be considered during model physics upgrade.

Future work will further evaluate the role of the cumulus scheme in HWRF forecasts with another case study (Hurricane Edouard, 2014) in comparison to extensive observations. Idealized HWRF simulations created by DTC with different versions of PBL schemes will be also analyzed to understand how different types of PBL schemes affect hurricane spin-up dynamics. Other types of physics that were not investigated in this project, such as microphysics schemes, will also be evaluated using a methodology similar to that used in this study.

6. References:

Arakawa, A., and C. M. Wu, 2013: A unified representation of deep moist convection in numerical modeling of the atmosphere. Part I. *J. Atmos. Sci.*, 70, 1977–1992.

Arakawa, A. and W. H. Schubert. 1974. Interaction of a cumulus cloud ensemble with the large-scale environment, Part I. *J. Atmos. Sci.*, 31, 674–701.

Biswas, M. K., L. Bernardet, and J. Dudhia, 2014: Sensitivity of hurricane forecasts to cumulus parameterizations in the HWRF model. *Geophys. Res. Lett.*, 41, 9113–9119, doi:https://doi.org/10.1002/2014GL062071.

Biswas, M. K., J. A. Zhang, E. Grell, E. Kalina, K. Newman, G. Grell, and L. Bernardet, 2019: Evaluation of the scale aware Grell-Freitas convective scheme with the HWRF model. *Weather and Forecasting*, in preparation.

Bryan, G., R. Rotunno, and Y. Chen, 2010: The effects of turbulence on hurricane intensity. 29th Conf. on Hurricanes and Tropical Meteorology, Tucson, AZ, Amer. Meteor. Soc., 8C.7, https://ams.confex.com/ams/pdfpapers/167282.pdf.

Braun, S. A., M. T. Montgomery, and Z. Pu, 2006: High-resolution simulation of Hurricane Bonnie (1998). Part I: The organization of eyewall vertical motion. *J. Atmos. Sci.*, **63**, 19–42.

Grell, G. A. and Freitas, S. R., 2014: A scale and aerosol aware stochastic convective parameterization for weather and air quality modeling, *Atmos. Chem. Phys.*, 14, 5233-5250.

Hack, J. J., and W. H. Schubert, 1986: Nonlinear response of atmospheric vortices to heating by organized cumulus convection. *J. Atmos. Sci.*, 43, 1559–1573.

Jones, S. C., 1995: The evolution of vortices in vertical shear: Initially barotropic vortices, *Quart. J. Roy. Meteor. Soc.*, 121, 821–851.

Kaplan, J., M. DeMaria, and J. A. Knaff, 2010: A revised tropical cyclone rapid intensification index for the Atlantic and eastern North Pacific basins. *Wea. Forecasting*, 25, 220–241.

Kaplan, J., C.M. Rozoff, M. DeMaria, C.R. Sampson, J.P. Kossin, C.S. Velden, J.J. Cione, J.P. Dunion, J.A. Knaff, J. A. Zhang, J.F. Dostalek, J.D. Hawkins, T.F. Lee, and J.E. Solbrig, 2015: Evaluating environmental impacts on tropical cyclone rapid intensification predictability utilizing statistical models. *Weather and Forecasting*, **30**, 1374-1396.

Kieper, M., and H. Jiang, 2012: Predicting tropical cyclone rapid intensification using the 37 GHz ring pattern identified from passive microwave measurements. *Geophys. Res. Lett.*, **39**, L13804, doi:10.1029/2012GL052115.

Kieu, C., V. Tallapragada, and W. Hogsett, 2014: Vertical structure of tropical cyclones at onset of the rapid intensification in HWRF model. *Geophys. Res. Lett.*, 41, 3298–3306, doi:10.1002/2014GL059584.

Kossin, J. P., and M. Eastin, 2001: Two distinct regimes in the kinematic and thermodynamic structure of the hurricane eye and eyewall. *J. Atmos. Sci.*, 58, 1079–1090.

Nolan, D. S., Y. Moon, and D. P. Stern, 2007: Tropical cyclone intensification from asymmetric convection: energetics and efficiency. *J. Atmos. Sci.*, **64**, 3377–3405.

Reasor, P. D., M. T. Montgomery, and L. D. Grasso, 2004: A new look at the problem of tropical cyclones in vertical shear flow: Vortex resiliency, *J. Atmos. Sci.*, 61, 3–22.

Riemer, M., M. T. Montgomery, and M. E. Nicholls, 2010: A new paradigm for intensity modification of tropical cyclones: Thermodynamic impact of vertical wind shear on the inflow layer. *Atmos. Chem. Phys.*, **10**, 3163–3188.

Rogers, R. F., P. Reasor and J. A. Zhang, 2015: Multiscale structure and evolution of Hurricane Earl (2010) during rapid intensification. *Mon. Wea. Rev.*, **143**, 536-562.

Rogers, R. F., P. Reasor, and S. Lorsolo, 2013: Airborne Doppler observations of the inner-core structural differences between intensifying and steady-state tropical cyclones. *Mon. Wea. Rev.*, 141, 2970–2991.

Schecter, D. A., 2015: Response of a simulated hurricane to misalignment forcing compared to the predictions of a simple theory. *J. Atmos. Sci.*, **72,** 1235–1260.

Smith, R. K., M. T. Montgomery, and S. V. Nguyen, 2009: Tropical cyclone spin-up revisited. *Quart. J. Roy Met. Soc.*, 135, 1321–1335.

Zhang, D.-L., and H. Chen, 2012: Importance of the upperlevel warm core in the rapid intensification of a tropical cyclone. *Geophys. Res. Lett.*, 39, L02806, doi:10.1029/2011GL050578.

Zhang, J. A., and W. M. Drennan, 2012: An observational study of vertical eddy diffusivity in the hurricane boundary layer. *J. Atmos. Sci.*, 69, 3223–3236.

Zhang, J. A., and M. T. Montgomery, 2012: Observational estimates of the horizontal eddy diffusivity and mixing length in the low-level region of intense hurricanes. *J. Atmos. Sci.*, 69, 1306–1316.

Zhang, J. A., and R. F. Rogers, 2019: Effects of parameterized boundary layer structure on hurricane rapid intensification in shear. *Mon. Wea. Rev*., in press.

Zhang, J. A., R. F. Rogers, P. D. Reasor, E. W. Uhlhorn, and F. D. Marks, 2013: Asymmetric hurricane boundary layer structure from dropsonde composites in relation to the environmental vertical wind shear. *Mon. Wea. Rev*., **141**, 3968–3984.

Zhang, J. A., R. F. Rogers, and V. Tallapragada, 2017: Impact of boundary layer parameterization on tropical cyclone rapid intensification: lessons learned from retrospective HWRF forecasts during physics upgrade, *Mon. Wea. Rev.* **145**, 1413-1426.

Zhang, J. A., F. D. Marks, M. T. Montgomery, and S. Lorsolo, 2011: An estimation of turbulent characteristics in the low-level region of intense Hurricanes Allen (1980) and Hugo (1989). *Mon. Wea. Rev.*, **139**, 1447–1462.

Zhang, J. A., F. D. Marks, J.A. Sippel, R.F. Rogers, X. Zhang, S.G. Gopalakrishnan, Z. Zhang, and V. Tallapragada, 2018: Evaluating the impact of improvement in the horizontal diffusion parameterization on hurricane prediction in the operational Hurricane Weather Research and Forecasting (HWRF) model. *Weather and Forecasting*, **33**, 317-329.